Bulk and Adsorbed Monolayer Phase Behavior of Binary Mixtures of Undecanoic Acid and Undecylamine: Catanionic Monolayers

ARTICLE *in* LANGMUIR · FEBRUARY 2011

Impact Factor: 4.46 · DOI: 10.1021/la1048198 · Source: PubMed

7 AUTHORS, INCLUDING:

Michael Janus Bojdys
Charles University in Prague
20 PUBLICATIONS **694** CITATIONS
SEE PROFILE

Stuart Clarke
University of Cambridge
132 PUBLICATIONS **1,863** CITATIONS
SEE PROFILE

Miguel A Castro
Universidad de Sevilla
74 PUBLICATIONS **830** CITATIONS
SEE PROFILE

Langmuir

ARTICLE

pubs.acs.org/Langmuir

Bulk and Adsorbed Monolayer Phase Behavior of Binary Mixtures of Undecanoic Acid and Undecylamine: Catanionic Monolayers

Chenguang Sun, Michael J. Bojdys,[‡] Stuart M. Clarke,* Lee D. Harper, and Andrew Jefferson

Department of Chemistry and BP Institute, University of Cambridge, Cambridge CB3 0EZ, United Kingdom

Miguel A. Castro and Santiago Medina

Instituto Ciencia Materiales de Sevilla-Departamento Química Inorgánica, CSIC-Universidad de Sevilla, Avenida Américo Vespucio s/n, 41092 Sevilla, Spain

Supporting Information

ABSTRACT: Differential scanning calorimetry (DSC) and X-ray powder diffraction (PXRD) have been used to determine the phase behavior of the binary mixtures of undecanoic acid (A) and undecylamine (B) in the bulk. In addition, we report DSC data that indicates very similar behavior for the solid monolayers of these materials adsorbed on the surface of graphite. The two species are found to form a series of stoichiometric complexes of the type AB, A_2B, and A_3B on the acid rich side of the phase diagram. Interestingly, no similar series of complexes is evident on the amine rich side. As a result of this complexation, the solid monolayers of the binary mixtures exhibit a very pronounced enhancement in stability relative to the pure adsorbates.

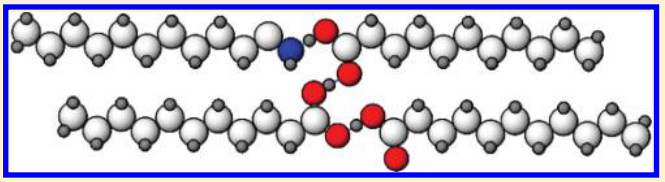

INTRODUCTION

The binary mixtures of carboxylic acids ($R-CO_2H$) and amines ($R-NH_2$) have been the subject of recent study. These combinations are particularly interesting because the two species can be thought to exchange a proton giving two ionic species ($R-CO_2^-$ and $R-NH_3^+$) that interact much more strongly than either of the original species. Alternatively, this interaction can be considered as an extreme form of hydrogen bonding. The formation of complexes can lead to unexpected behavior in the mixtures, for example, particularly stable layers; hence, the identification and exploitation of such synergy can be important commercially. Some workers, using mainly spectroscopic techniques, have reported evidence for a series of complexes between these types of acid and amine species. These complexes include the simple 1:1 mixture acid/base (AB) complex, but a number of others have also been proposed, such as A_2B, A_3B, and so forth, on the acid rich side of the phase diagram.[1−6] These complexes and molecular associations are in addition to the more usual acid dimerization observed in the crystals of pure acids arising from hydrogen bonding between two acid groups, referred to here as A_2.

The structure of such complexes is interesting, and models have been proposed to account for the extended association of several acid molecules with a single amine, such as that illustrated in Figure 1. The molecular structure of the molecules involved is reported to be significant in determining which of the possible complexes are favored. In systems with tertiary amines, it is reported that complexes of the type A_3B predominate. When bulky substituents are present at the α position on the carbon atom to the carboxylic acid headgroup, then the 2:1, A_2B, complex can be favored.[7]

There is now a fairly extensive body of evidence concerning the formation of these complexes in short chain acids and amines using a variety of techniques including IR, NMR, small-angle X-ray scattering, melting curves, viscosity, surface tension, and conductiometric and volumetric methods.[2,6−8] Many of these systems have been considered in the presence of water, ternary systems, partly because mixtures of cationic and anionic surfactants are particularly important.[9] Equimolar mixtures of alkanoic acid and an alkylamine form a salt called a catanionic surfactant,[8] reflecting the importance of their surface behavior.

Most relevant here are studies on binary mixtures of acids and amines with longer alkyl chains such as heptanoic acid and heptylamine[8] and the hexyl[10] and octyl derivatives.[11] Again, the majority of studies involve ternary systems with water, and the measurements have all been made at, essentially, room temperature. A variety of spectroscopic techniques has been used to show that an A:B complex forms for these longer alkyl species. With excess acid, more complexation is observed, for example, A_3B is formed. However, the A_2B complex does not appear to be formed in these cases.

Interestingly, additional complexes are not found with excess amine; the amine rich complexes AB_3 and AB_2 do not appear to be formed. Recent IR results and ab initio calculations by

Received: December 3, 2010
Revised: January 31, 2011
Published: February 28, 2011

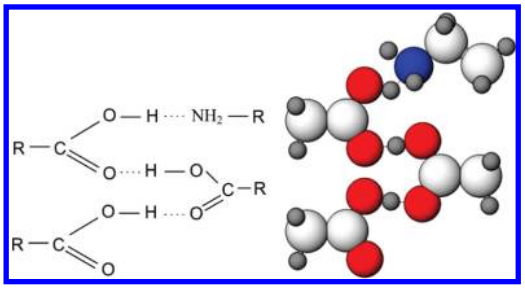

Figure 1. Schematic illustration of a possible coordination of several acid molecules to a single amine giving rise to extended A_nB complexes. Blue, nitrogen; red, oxygen; light gray, carbon; dark gray, hydrogen.

Paivarinta et al.[12,13] have suggested that these complexes are relatively unstable.

Monolayers. The formation of solid monolayers that adsorb from the liquid to graphite have been observed for a wide variety of simple molecules including linear alkanes,[14−17] alcohols,[18−25] carboxylic acids,[26−28] and amines.[29] Carboxylic acids have also been reported to adsorb solid monolayers from solution. The two pure materials of interest here, undecanoic acid and undecylamine, have both been demonstrated to form solid monolayers adsorbed from their pure liquids. Hence, there is considerable interest in identifying the phase behavior of these binary mixtures when adsorbed to the surface of graphite, particularly considering the rich potential for complex formation with acid/amine complexes considered here. Surface complexation and molecular compound formation have been reported for other systems such as linear alcohols.[22]

In this work, we address the phase behavior of binary mixtures of undecanoic acid and undecylamine both in the bulk and in the adsorbed monolayer with particular interest in the complexation behavior and the enhanced stabilization behavior this can give rise to.

EXPERIMENTAL SECTION

The procedures for using differential scanning calorimetry (DSC) to measure and identify phase transitions in both bulk and adsorbed materials have been reported[30,31] elsewhere. In this work, a Perkin-Elmer Pyris 1 power compensation DSC instrument at the BP Institute, University of Cambridge has been used. In outline, the small energy changes of a sample relative to an empty reference can be used to identify phase transitions in a sample. The transitions in bulk materials are relatively large and much more straightforward to measure than the significantly smaller transitions that occur in a monolayer. However, both bulk and monolayer transitions can now be measured routinely when high specific surface area substrates are used which provide a relatively higher proportion of monolayer signal.

DSC is a dynamic technique, and for simple first order phase transitions, such as melting in the bulk of a pure sample, the peak position observed in the DSC thermograms is not at the transition temperature. Rather the transition temperature occurs at the "onset"[32] of the peak, essentially the temperature when the heat capacity begins to rise significantly from the baseline, usually estimated by an extrapolation on the low temperature side of the DSC peak. However, it can also be shown that in some situations the peak position is more representative of the transition temperature than the onset. This is the case for the liquidus of an eutectic, in heating, and for second order transitions. While it is fairly straightforward to accurately locate the position of a peak in the thermograms, the position of the "onset" is more difficult to determine, particularly if several peaks are close to one another. Where possible, we have determined the "onset" temperature, but peak positions have been reported where this has not been reliable, or where we have a bulk liquidus.

The DSC instrument has been calibrated for temperature using indium and heptane, and for enthalpy by indium following standard procedures recommended by the manufacturer. Pure organic molecules can also be used as calibrants with an error reflecting their purity.

The diffraction experiments were performed on the I11 instrument at the DIAMOND light source, synchrotron facility. This is a powder diffractometer with a position sensitive multidetector allowing rapid counting and hence the facility to sweep the temperature a phase diagram readily. The device was calibrated for wavelength and angle using a silicon standard. The samples were held in glass capillaries as discussed in more detail below and rotated to achieve more effective powder averaging.

A "Cryostream" was used to control the sample temperature using a stream of temperature controlled nitrogen gas blowing onto the sample. The absolute temperature of the sample was not directly accessible during X-ray scans. Comparison of transitions in X-ray powder diffraction (PXRD) and DSC identified that the PXRD transition temperatures are slightly higher than those of DSC, which we attribute to the thermal gradients in the PXRD system.

Sample Preparation. In this work, we have employed several samples of undecanoic acid ($CH_3(CH_2)_9COOH$) and undecylamine ($CH_3(CH_2)_{10}NH_2$). The sample purities are as follows: acid 99.6% determined by titration and 99.0% by GC, and the amine 99.8% determined by titration and 100.0% by GC. It is difficult to determine the nature of these small quantities of impurity. However, a typical acid sample gave an elemental C/O ratio of 5.54 ± 0.03 (theoretical ratio 5.5) (average of two samples determined by us) within 0.8% of the expected value (elemental analysis determines the C and H content, the oxygen content determined from the mass balance). A fresh amine sample gave a C/N ratio of 10.90 within 0.9% (theoretical ratio 11.0) of the expected value. NMR data collected by us were quantitatively consistent with the desired structures.

The most significant purity issue concerns the reaction of the amine with CO_2 from the air to produce carbamates.[33,34] Initial measurements indicted that this could give rise to small amounts of reaction and hence some uncertainty in the results. To be sure that this reaction was eliminated, the following procedures were followed to completely avoid any contact with the air for all the measurements reported here (PXRD and DSC). The acid samples, which were not air sensitive, were weighed out into small vials. These acid samples and the unopened amine stock were transferred to a nitrogen glovebox. All samples/items placed in the box were evacuated and exchanged with nitrogen gas at least four times (approximately 1.5 h) to ensure no CO_2 could be present. The correct amount of amine was added to the vials by volume using a Hamilton microsyringe. The bulk samples were warmed to the liquid state with a small heat gun to ensure good mixing. These mixtures were transferred to glass capillaries: liquid samples by syringe and solid samples by grinding into powders and transferring them to the capillary. The capillaries were temporally sealed with Apiezon black wax melted into place with a hot air gun and then removed from the glovebox and sealed permanently with a small torch/stove lighter. The sealed capillaries were kept in airtight containers for transfer to the synchrotron facility, only being removed just prior to being investigated, but still within the sealed glass capillaries. These approaches are based on techniques routinely used for highly reactive air sensitive materials in the Inorganic Sector at the Department of Chemistry, Cambridge University. DSC samples were similarly prepared in a high quality glovebox and hermetically sealed in the aluminum DSC sample pans using a crimper in the glovebox. They were kept in a nitrogen atmosphere in transit from the glovebox to the DSC instrument and only removed immediately prior to running in the DSC instrument. It was found that a few samples were not

dx.doi.org/10.1021/la1048198 |*Langmuir* 2011, 27, 3626–3637

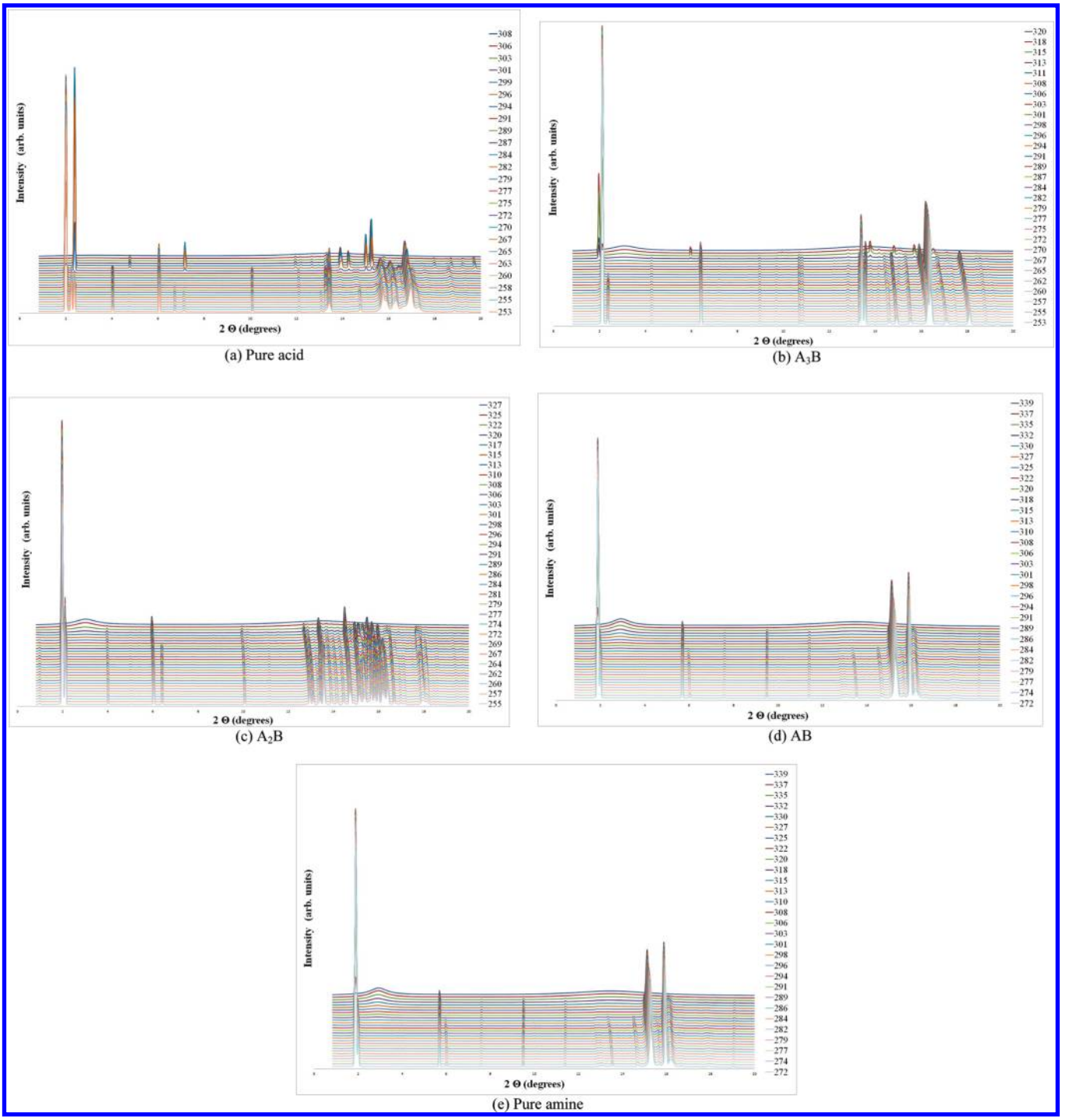

Figure 2. Temperature dependence of the diffraction data from bulk mixtures of undecyl amine and acid at compositions corresponding to (a) pure acid, (b) 0.75 mol fraction acid (A_3B), (c) 0.67 mol fraction acid (A_2B), (d) 0.50 mol fraction acid (AB), and (e) pure amine.

well sealed; however, this was readily detected by the presence of a white deposit on the pans and data from such samples was discarded. It was found that the amine was implicated in preventing this sealing of the aluminum. To prevent this problem, a number of approaches were investigated including prefreezing the DSC pans before adding the sample and careful positioning of the samples in the pans. However, the most effective method was considered to be to use alternative steel pans, sealed by rubber O-rings. These have slightly poorer thermal conductivity but did not show signs of leakage. The composition of the DSC sample mixtures could be well controlled in the glovebox in this approach; however, the total amount of each mixture added to the DSC pans could not be determined as precisely, due to the precision of the balance in the glovebox (error estimated as approximately ±5 mg). Hence, although the phase behavior and transition temperatures of the samples determined here should be accurate, an estimate of the transition enthalpy (estimated from the areas of the DSC transitions) is not considered to be as reliable. Not more than 5 mg of adsorbate per sample was used, in order to keep thermal lag low, and samples were annealed at 353 K for 24 h.

dx.doi.org/10.1021/la1048198 |*Langmuir* 2011, 27, 3626–3637

It is also possible that the alkyl amine and alkyl carboxylic acid could react to give an amide. To address this issue, elemental analysis was also taken of a 0.50 mol fraction mixture after heating and cooling well above the melting point and after all measurements have been made with it. This analysis confirmed that no reaction had occurred (to form the amide) and this composition remained a mixture of the acid and the amine (73.6% C, 13.25% H, and 4.01% N which compares well with the expected elemental ratios of 73.45% C, 13.17% H, and 3.92% N). Hence, we conclude that there is no evidence of a reaction to form the amide. Usually amide formation requires activation of the acid group by formation of the acyl chloride.

The use of DSC for the investigation of monolayer adsorption has been reported previously. The samples are prepared with a small known mass of the graphite substrate in the DSC pans (approx. 10 mg). The graphite has been cleaned under vacuum at 623 K before use, and its specific surface area determined by nitrogen isotherm (approximately 30 m^2/g). The samples are annealed at elevated temperature prior to use. The amount of adsorbates added corresponds to approximately 40 monolayers.

Previous work has indicated that carboxylic acids exhibit preferential adsorption of the longer homologue. In this experiment, both components are C11 alkylated species; hence, we do not expect the surface composition to vary significantly from that of the bulk. As will be shown below, this is partly supported by the observation of features in the monolayer phase diagram occurring at the same composition as similar features in the bulk material.

RESULTS AND DISCUSSION

Bulk Phase Behavior. Here we present our proposed phase diagram and then give the experimental evidence in support of this conclusion. The proposed phase diagram of the bulk acid/amine combination is given in Figure 4.

In outline, we propose that there are three stoichiometric compositions: 0.50 mol fraction acid (AB complex), 0.67 mol fraction acid (A_2B complex), and 0.75 mol fraction acid (A_3B complex). The pure acid and the A_3B complex phase separate. The A_3B and A_2B complexes coexist and do not mix in the solid state, as do the A_2B and AB complexes. The AB complex and the pure amine also coexist and do not mix in the solid phase. The A_3B complex melts incongruently to give the A_2B complex. The amine and AB complex also do not mix in the solid phase. Some materials show additional solid phases with changing temperature.

Figure 2 presents the temperature dependence of the diffraction data from bulk mixtures of undecylamine and acid at compositions corresponding to (a) pure acid, (b) 0.75 mol fraction acid (A_3B), (c) 0.67 mol fraction acid (A_2B), (d) 0.50 mol fraction acid (AB), and (e) pure amine.

Figure 2a shows that there are three solid phases of the pure acid, denoted A(III) for lowest temperatures, and A(II) and A(I) for highest temperature phase. The A(III) and A(II) phases have very similar peak positions, and they only differ in the relative peak intensities. These may arise from subtle changes in the structure with temperature and A(III) and A(II) may be very similar structures and not separate phases. Here we have delineated them as they have slightly different diffraction patterns.

The melting point of the pure acid, where the sharp peaks completely disappear to be replaced by the broad scattering of the liquid, is found to be 308 K, somewhat higher than the literature melting point of 301 K. We attribute this difference to the thermal gradients in the experimental diffraction system, explained above.

Table 1. Positions of the Characteristic Peaks of the Phases

phase	peak positions (2θ)
acid (I), high temperature	2.39, 4.78, 7.18, 13.92, 14.20, 15.26, 16.81
acid (II)	2.00, 4.00, 6.05, 10.1, 13.4
acid (III)	2.00, 2.25, 2.35, 4.00, 6.05, 10.1, 13.4
A_3B	2.116, 6.38, 13.4, 16.34
A_2B	1.99, 6.01, 13.41
AB	1.88, 5.67, 15.30, 15.95
amine	2.01, 4.04, 6.07, 8.14, 14.30, 15.10, 16.92

The position of peaks characteristic of each of these phases are given Table 1. The positions of the three lowest order diffraction peaks for the high temperature phase of the acid (2.39°, 7.18°, 13.92°) are in good agreement with those calculated from the Cambridge Structural Database entry for the high temperature phase of undecanoic acid[35,36] (2.35°, 7.13°, 13.92°). Several alkyl carboxylic acids have been reported to form more than one solid crystal phase close to the bulk melting point. The bulk crystal structures have been reported previously and consist of molecular dimers. It has also been established that the dimeric form of these molecules persists into the liquid state as evident in various colligative properties.[27,28]

Figure 2e indicates that the amine forms a single solid phase. The peaks characteristic of this amine phase are given in Table 1. The melting point is identified as the temperature where these solid peaks disappear; as indicated below, this is again slightly higher than that determined by DSC suggesting some modest thermal gradients in the system.

Similar patterns from the other stoichiometric compositions are given in Figure 2, and the principle characteristic peaks of each phase are given in Table 1. It is noted that in some cases small contributions from other phases appear in the patterns where the experimental compositions are not precisely those of the stoichiometric compositions.

In particular, Figure 2d for the AB composition has a small amount of the A_2B phase, and Figure 2c, the A_2B composition, has a small amount of A_3B present. The A_3B composition, Figure 2b, transforms to the A_2B phase (peaks at 2.08, 6.01) just prior to melting, indicating incongruent melting.

There is a weak peak in the A_3B composition data at 2.36° that disappears at approximately 300 K which could arise from a small amount of the A(III) phase. At a composition of 0.30, there is a change on heating from two very closely placed peaks at 5.9° and 6.0° to a single peak at 6.0°. However, there is no evidence of similar subtle changes in the diffraction data at adjacent compositions. As discussed below, these features are attributed to a solid−solid phase transition that is more evident in the calorimetry data.

Figure S1 of the Supporting Information gives the diffraction patterns from points in the phase diagram corresponding to the coexisting phases: (a) A(III)/A_3B, (b) A(II)/A_3B, (c) A(I)/A_3B, (d) A_3B and fluid, (e) A_3B/A_2B, (f) A_2B and fluid, (g) A_2B/AB, (h) AB and fluid, (i) AB/amine, and (j) AB and fluid. Representative peaks at low angles from the particular phases are indicated in the figure.

Figure 3a presents a typical DSC thermogram from pure undecanoic acid. This figure illustrates the main acid melting peak with an extrapolated onset at approximately 303.1 K and

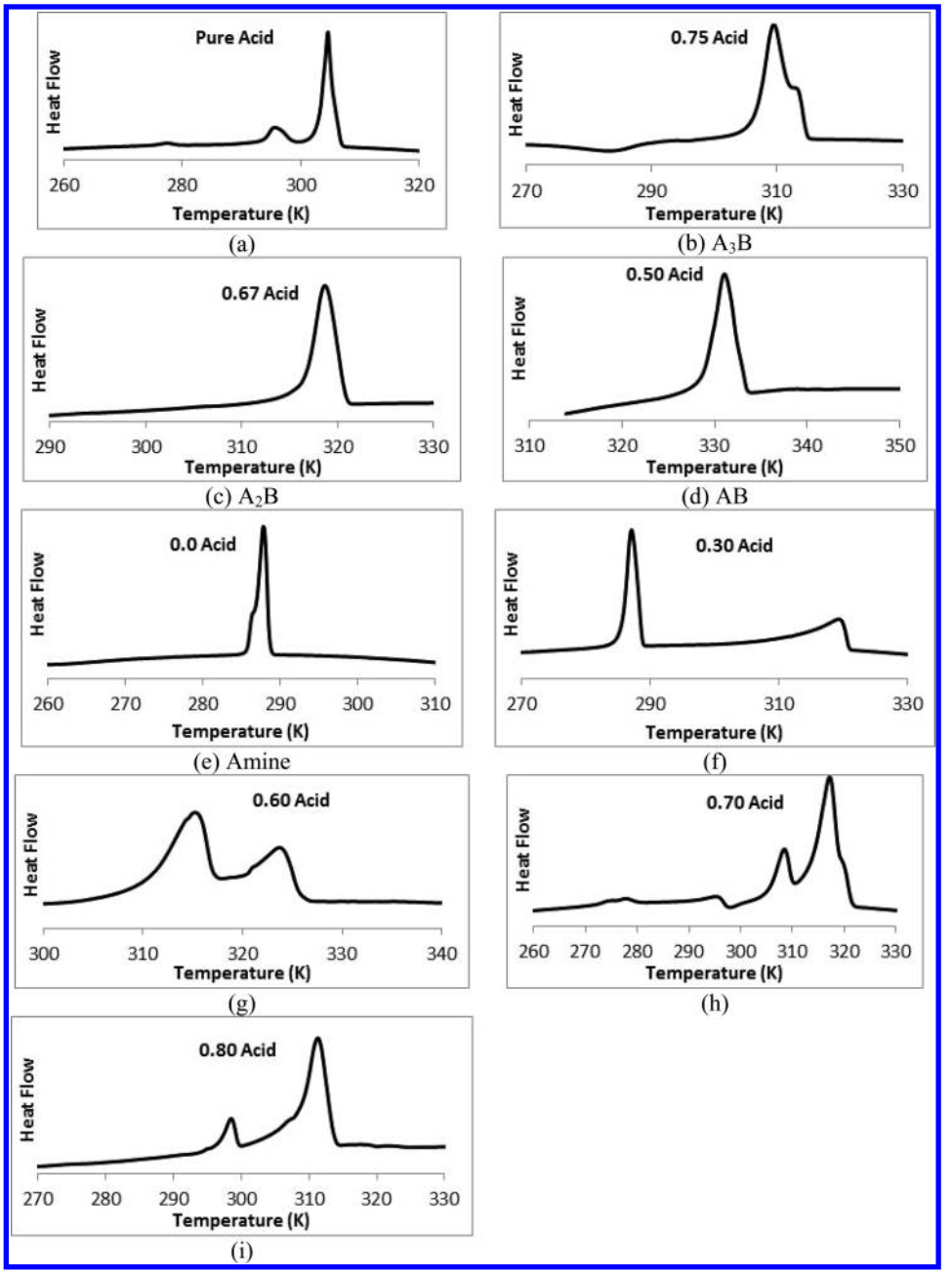

Figure 3. DSC thermograms from (a) pure undecanoic acid, (b) A_3B, (c) A_2B, (d) AB, and (e) pure undecylamine. (f−i) Mixtures with intermediate compositions as discussed in the text.

additional solid−solid phase transition peaks at approximately 276 and 294 K. This behavior is in good agreement with the PXRD data above and the melting points quoted by the supplier and literature, 301−304 K and 301.6 K, respectively.[37,38] Solid−solid phase transition[35] for this acid has been reported previously to be at 293.7 K.[38] Hence, it is the high temperature form that melts at 303.1 K. The temperatures of the transitions determined by PXRD are somewhat higher than those from DSC, as noted above, which we attribute to thermal gradients in the PXRD experiment.

Figure 3e presents similar data for the DSC pure amine. This data indicates the large amine melting transition with a peak at approximately at 289 K. This is in the range of melting point given by the supplier (288−290 K) but somewhat below the literature value of 293.2 K.[37] This data also indicates a weak shoulder to the low temperature side of the peak, suggesting that there may be a solid−solid phase transition just prior to the bulk melting point. However, this low temperature phase would be very hard to observe with diffraction with such a small temperature range of stability.

Figure 3b−d illustrates DSC thermograms from the other stoichiometic complexes. The DSC thermogram in Figure 3d (AB) indicates a single bulk phase at this composition, which melts at approximately 327 K. Significantly, this material melts at a much higher temperature than either of the pure acid or amine. This is a clear indication of the strong interaction and synergy of these materials and suggests molecular compound/complex formation. The DSC thermogram in Figure 3c for the A_2B

dx.doi.org/10.1021/la1048198 |*Langmuir* 2011, 27, 3626–3637

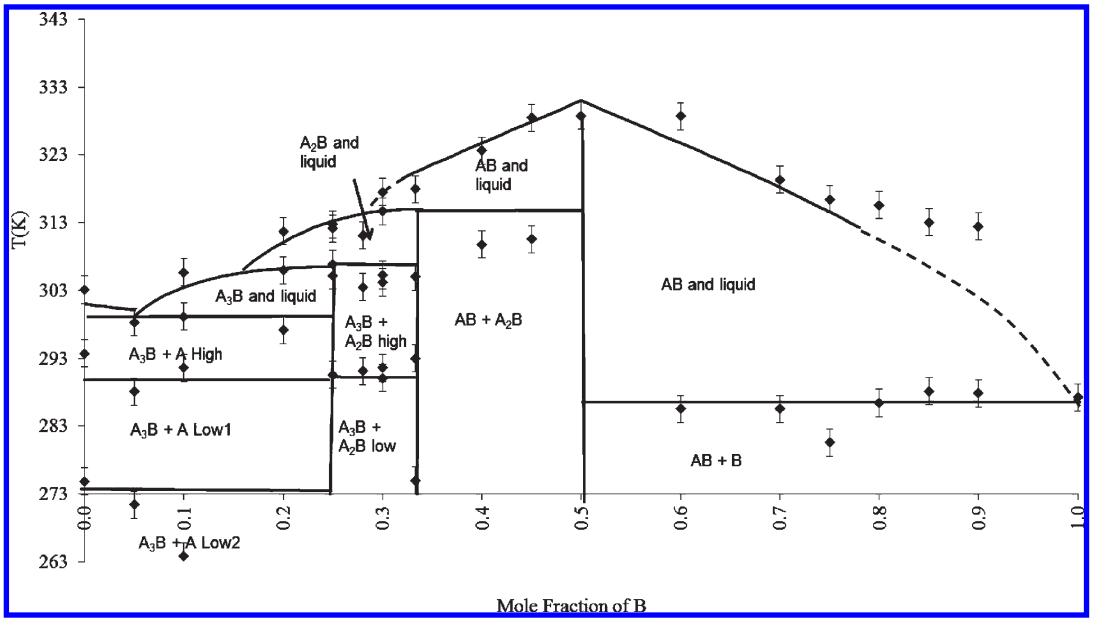

Figure 4. Experimentally determined phase diagram for bulk undecylamine and acid.

composition exhibits a single peak at its melting point of approximately 315 K. Figure 3b shows the DSC thermogram for the A_3B composition which exhibits two large transitions at approximately 308 and 313 K. These are attributed to the $A_3B \rightarrow A_2B$ transition and A_2B subsequent melting. There is a much weaker, exothermic feature at approximately 288 K attributed to a solid−solid phase change from a A_3B low temperature phase to a A_3B higher temperature phase. Some of the X-ray diffraction patterns also exhibit a feature at approximately these temperatures however, they are very weak.

The DSC thermogram in Figure 3f for the 0.30 mol fraction acid composition exhibits behavior typical of a phase separating system with a sharp eutectic invariant peak at 287 K and the liquidus at approximately 277.5 K. This is in very good agreement with the PXRD. Similar eutectic behavior is observed in Figure 3i at 0.80 mol fraction where the pure acids and the A_3B complex do not mix.

DSC thermograms in Figure 3g and h exhibit two large peaks around 314 and 323 K at 0.6 (g) and 308 and 317 K at 0.7 (h) . The low temperature transitions are attributed to the phase transitions from $A_3B \rightarrow A_2B$ and $A_2B \rightarrow AB$, respectively. The higher temperature transitions are the melting of the high temperature phases.

In the 0.70 mol fraction sample, there is the weak transition at approximately 288−293 K, attributed to the A_3B solid−solid phase transition. There also is some evidence of a very weak transition around 273 K which is found to be dependent upon the rate of cooling in DSC. This is most evident when the sample is cooled slowly. We note that the X-ray diffraction measurements were collected with relatively fast cooling and we do not expect this to be evident in the scattering patterns. This behavior is often typical where the relative rates of nucleation of different phases are important. These last two transitions appear across the 0.67−0.75 mol fraction region of the phase diagram, also indicating that these features arise from the A_3B complex.

Figure 3i at 0.8 mol fraction has two principal peaks at approximately 297 and 313 K. These are the eutectic invariant and melting temperatures, respectively, of the sample at this composition.

Figure 4 presents the experimentally determined phase diagram for undecanoic acid and undecylamine based on the data given above. The transition temperatures have been based on the calorimetry data, rather than those determined by PXRD due to the thermal gradients in the diffraction experiments. The error bars in this figure are an estimate of the temperature stability over the period of the measurements.

It is found that the pure acid, in either its low or high temperature phases, forms a eutectic mixture with the A_3B complex. The composition variation of the melting point of the mixtures on the acid rich side of the phase diagram determined by DSC indicates a eutectic invariant, at a temperature of approximately 298 K with the eutectic composition at approximately $x_A = 0.1$.

The behavior at higher compositions of amine strongly suggests peritectic behavior and incongruent melting of A_3B to A_2B prior to melting. On the amine rich side of the phase diagram, the data indicate eutectic, phase separation behavior with the eutectic invariant at essentially the pure amine melting point.

This work clearly supports the extensive formation of stoichiometric complexes by an alkyl carboxylic acid and an alkyl amine, previously indicated by spectroscopy and other techniques for closely related systems.[1−6] Interestingly, three complexes are observed: AB, A_2B, and A_3B, but no higher members (e.g., A_4B) and none on the amine rich side of the phase diagram. The system studied here slightly differs from some other earlier work where particular members (e.g., A_2B) were not observed. As expected, the complexes are relatively much more stable in the solid state than the pure materials, particularly reflected in the very high melting point of the AB complex. It is also interesting that the complexes exhibit peritectic behavior decomposing to a lower stoichiometry complex prior to melting.

The transitions in the experimental phase diagram can be compared with theoretical models based on the solid phase mixing behavior and the extent of complexation in the liquid.[39]

dx.doi.org/10.1021/la1048198 |*Langmuir* 2011, 27, 3626–3637

Table 2. Experimental Values of the Bulk and Monolayer Melting Points of the Undecylamine and Undecanoic Acid

pure cmpd	experimental melting point (K)
bulk	
A	303.1
B	289.1
monolayer	
A	327.0
B	307.5

Table 3. Parameters Used for the Calculations Used to Model the Bulk and Monolayer Phase Diagrams

cmpd	melting point (K)	enthalpy of fusion (kJ/mol)
bulk complexes		
A B	331	58
A_2B	315	25
A_3B	307	95
monolayer phases		
A	326	55
AB	375	40
A_2B	352	4.8
A_3B	341	3.0

An outline of composition dependence of these transitions is briefly discussed in the Supporting Information for a number of key thermodynamic transitions. A comparison of the experimental data and these models is given in Figure 4. The parameters used in these calculations are given in Tables 2 and 3. The enthalpy of the acid melting has been taken to be twice the literature value of the enthalpy of melting (25.1 kJ/mol) in these calculations due to the dimerization. The extent of dissociation of AB in the liquid cannot be unambiguously determined from the gradients of the melting points with composition due to the scatter in the experimental data; however, it appears that the model where the AB complex remains in the liquid state is more representative than the model where the components dissociate on melting. The calculations in the region of the A_2B and A_3B complexes illustrated in Figure 4 are the model where dissociation occurs in the liquid. There is significant uncertainty in these calculated parameters, partly arising from the scatter in the experimental transition temperatures and the simplicity of the thermodynamic models used. In particular, the value of the A_3B complex enthalpy seems rather high and arises from fitting a single point on the phase diagram. However, the general form of the phase behavior is consistent with the proposed phase diagram.

Monolayer Behavior. Figure 5 presents thermograms from acid/amine mixtures in the presence of graphite where the temperature region just above the bulk melting point is highlighted. The formation of solid monolayers of adsorbed pure carboxylic acids and pure amines has been reported previsously[18,26−29,40] and confirmed by diffraction studies. Monolayers formed at high coverage (well above one equivalent monolayer), approximately 40 monolayers, coexist with bulk liquid. For the temperature region just above the bulk melting point, the system is considered to consist of a single solid monolayer of adsorbate and the rest of the adsorbate is liquid. This is significantly different from those adsorbed at submonolayer coverage where the monolayer melting point is below the bulk melting point (often approximately 0.75 of the bulk melting point). At higher coverage, the monolayer is found to melt at temperatures above the bulk value, as seen here. There is some evidence that this difference may be due to a compression of the layers on increasing the coverage. The monolayer formation is evident in the DSC thermograms by the weak transition at temperatures above the bulk melting point that are only evident in the presence of the substrate, as illustrated in Figure 5a for representative compositions.

The monolayer melting transition of the pure acid has been previously identified in DSC thermograms, and its assignment confirmed by other techniques, such as incoherent neutron scattering and diffraction. It is evident from the thermograms in Figure 5a that all the different compositions measured have a similar transition that can be identified in all compositions across the phase diagram of the binary mixtures adsorbed on graphite and are, therefore, also assigned to monolayer melting. The variation in temperature of these solid monolayer melting points is illustrated in Figure 5b. In some cases, there are additional weak peaks identified in the thermograms that could also arise from transitions of a monolayer. Other monolayer systems exhibit similar additional transitions, arising from solid−solid phase transitions or layering, such as alcohols and amides.

Significantly, we note that the monolayer peaks in Figure 5b essentially follow the bulk melting point across the phase diagram, but just displaced to higher temperatures. This strongly suggests that the surface phase behavior essentially mimics that of the bulk complexation. The composition of the pronounced maximum in melting point somewhere in the region of 0.5−0.6 mol fraction suggests that the surface composition is essentially that of the bulk and there is minimal preferential adsorption which can be represented by a small preferential adsorption equilibrium constant of no more than 1.15. The essentially equivalent adsorption of these species is not unsurprising, given that preferential adsorption is usually a function of increasing alkyl chain length.[21,22,28,41−47] Here both species have equal alkyl chain lengths and so are expected to adsorb equally strongly on this surface.

The degree of monolayer melting temperature elevation relative to the bulk is most extreme at the AB composition, indicating formation of the surface AB complex, like the bulk. This enhancement in monolayer stability over either of the two pure components is most marked. Understanding and exploiting this synergy could have important implications both academically and commercially. The amine rich side of the monolayer phase diagram appears to show a smooth temperature variation, like the bulk. On the acid rich side of the diagram, we clearly see a number of features indicative of the surface equivalent of the bulk complexation behavior. For example, the depression of freezing point at low amine mole fractions suggests eutectic behavior, and the gradual increase in monolayer melting point with increase in acid is also an echo of the bulk complexation behavior. We compared the experimental data to the complexation models in analogy to the bulk samples above, where the A_2B and A_3B complexes dissociate on melting. Given the significant scatter in the data and the uncertainty of the extent of complexation in the liquid state, we consider that the lines in Figure 5b are essentially guides to the eye but do illustrate that the proposed phase diagram is reasonable. Although we consider that the surface behavior is a series of complex formations, it is extremely difficult

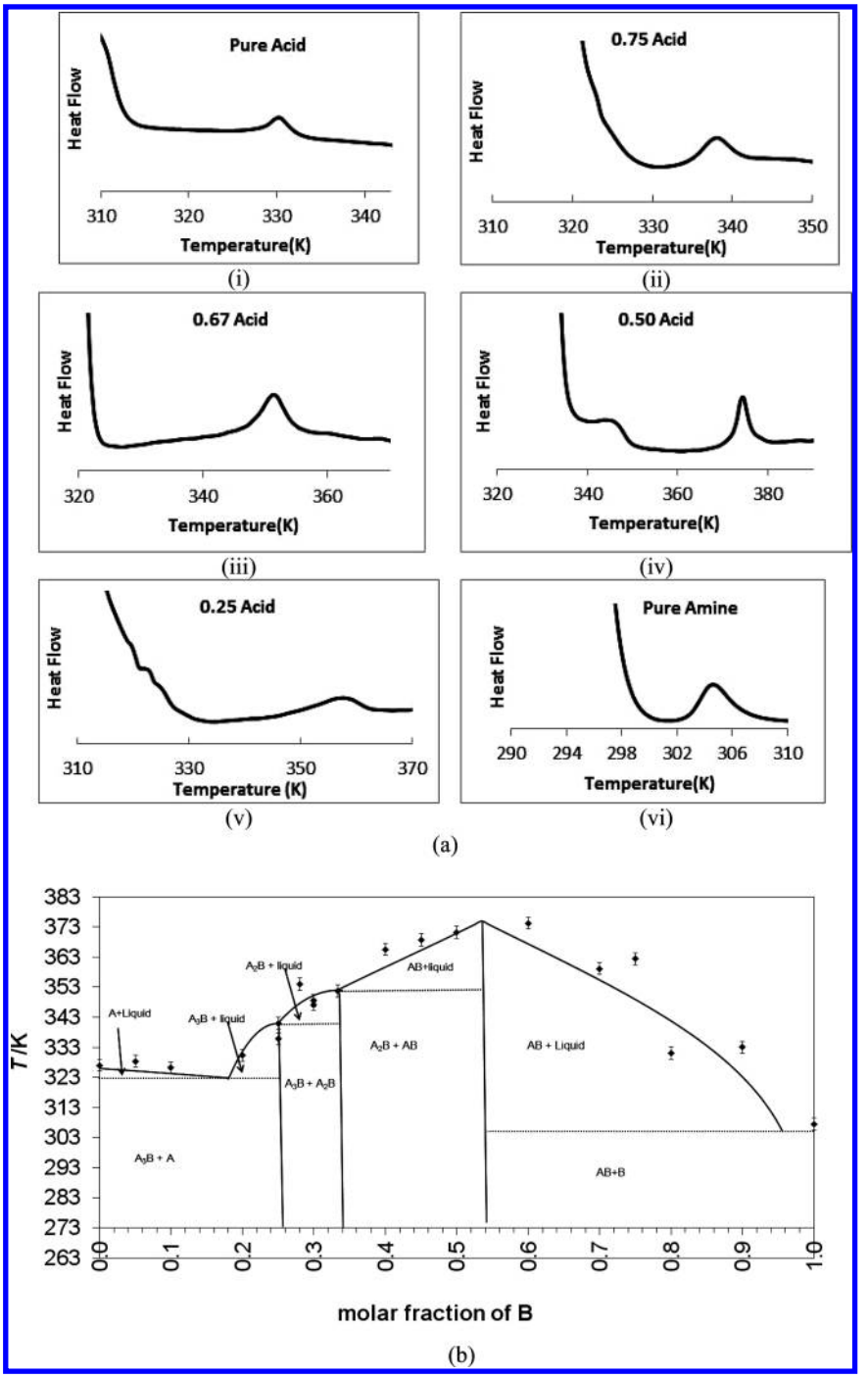

Figure 5. (a) Thermograms from acid and amine mixtures adsorbed on graphite indicating the transitions from the adsorbed monolayer. (b) Monolayer melting point variation with bulk composition. Lines represent complexation models discussed in the text.

to be conclusive. This uncertainty has several origins, most significantly that the monolayer melting transitions are extremely weak. The other transitions (e.g., eutectic invariants, peritectic transitions, etc.) which one would normally see in the bulk cannot be observed here. Diffraction in the presence of much larger quantities of bulk liquid adsorbate is also generally very difficult. The formation of the A_2B and A_3B surface complex is also unclear and can only be implied by the similarity of the variation in monolayer and bulk melting points with composition over this region of the phase diagram. The data also reflect a significant uncertainty on the monolayer melting temperatures, particularly on the amine rich side of the phase diagram. This is partly attributed to the very weak nature of the monolayer transitions.

The structural nature of these monolayers is an interesting issue, and we have, with colleagues in Belgium, attempted to make STM images of these monolayers. However, these have not yet been successful. Diffraction studies at these high coverages are also a significant challenge with the bulk liquid scattering obscuring all but the most intense features of the monolayer. We have some preliminary synchrotron diffraction data (not shown) at submonolayer coverages that does indicate formation of a solid

dx.doi.org/10.1021/la1048198 |*Langmuir* 2011, 27, 3626–3637

monolayer AB complex that melts at a similar temperature to the high coverage monolayer melting point given here. However, a full study of the submonolayer behavior represents a significant additional project that we intend to undertake in the next few years. In this submonolayer regime, it might be possible to distinguish coexistence of the different monolayer complexes. However, this would require that diffraction peaks characteristic of each phase are well separated to allow this analysis to be made. Usually, the characteristic peaks of adsorbed monolayers of molecules with similar alkyl chain lengths occur at very similar scattering angles. Combined with the inherently broad nature of 2D line shapes, this represents a significant challenge and has only been successfully achieved in very few cases.

It is possible to speculate on the molecular packings in the monolayer of these complexes. One key feature of monolayer of alkyl species is the dominant lamellar packing of the alkyl chains which also can accommodate additional strong hydrogen bonding, such as with the alcohol monolayers,[24,25] carboxylic acid monolayers,[27] and amide monolayers.[48] Hence, we expect similar cooperative arrangements in this case. The details of packing in mixed 2D layers is complex and has been discussed previously.[21,22,28,41,42,45,46,49] The essential features in many cases echo bulk rules and combine symmetry and molecular size. However, these rules are readily broken in unexpected ways, as reflected by the ideal mixing or complexation behavior of very similar alcohol mixtures.[21,22] Hence, we are reluctant to propose particular monolayer packing arrangements at this stage.

■ CONCLUSIONS

This work has provided the complete bulk phase diagram of the binary mixing behavior of undecylamine and undecanoic acid. The rich phase behavior has been fully presented and includes three solid complexes, several additional low temperature solid phases, and a variety of melting behaviors including eutectic, peritectic, dystetic, and incongruent melting, previously unreported. The results are in qualitative agreement with related materials in the literature, but this is the first study of this particular combination of materials. It also is one of the few studies exploiting diffraction and calorimetry in this area. More significantly, this is a unique example of such complexation behavior in a solid monolayer adsorbed on the surface of graphite from the liquid. The variety of complexes formed is very interesting and is somewhat more complex than might normally have been expected from binary mixtures of surfactants in detergency where the mixing behavior might be assumed to be represented by a single regular solution parameter. The greatly enhanced stability of the complexes (particularly the AB solid monolayer) over the monolayers of the pure materials (of some 50 K) represents a great opportunity for the formation and exploitation of strong physisorbed monolayers in a variety of applications such as lubrication and detergency.

■ APPENDIX I: THERMODYNAMIC DERIVATIONS AND CALCULATIONS

(A). Melting of a Single Component in a Mixture. For a pure material at its melting point, the chemical potentials of the species must be the same in the solid and the liquid state.

$$\mu_A(s) = \mu_A(l)$$

If there is no mixing in the solid phase but ideal mixing in the liquid, then we can write for these chemical potentials

$$\mu_A(s) = \mu_A^\circ(s)$$

$$\mu_A(l) = \mu_A^\circ(l) + RT\ln(X_A)$$

Giving

$$\mu_A^\circ(s) = \mu_A^\circ(l) + RT\ln(X_A)$$

where $\mu_A^\circ(s)$ and $\mu_A^\circ(l)$ are the chemical potentials of the pure species of A in the solid and liquid states, respectively, at T, the absolute temperature, and X_A, the mole fraction of "A" in the liquid. On rearranging, we find:

$$\mu_A^\circ(l) - \mu_A^\circ(s) = -RT\ln(X_A)$$

$$\frac{\mu_A^\circ(l) - \mu_A^\circ(s)}{T} = -R\ln(X_A)$$

$$(X_A)\left(\frac{\Delta\mu_A^\circ}{T}\right)_{T=T} = -R\ln(X_A) \quad (1)$$

At the melting point of the pure material, $X_A = 1$, and temperature $T_{m,A}$, we have

$$\mu_A^\circ(l) - \mu_A^\circ(s) = 0$$

$$\frac{\mu_A^o(l) - \mu_A^o(s)}{T_{T=T_{m,A}}} = 0\left(\frac{\Delta\mu_A^o}{T}\right)_{T=T_{m,A}} = 0 \quad (2)$$

Combining eqs 1 and 2 gives

$$\left(\frac{\Delta\mu_A^\circ}{T}\right)_{T=T} - \left(\frac{\Delta\mu_A^\circ}{T}\right)_{T=T_{m,A}} + R\ln(X_A) = 0$$

Using the Gibbs−Helmholtz relation, we find:

$$\left(\frac{\Delta\mu_A^\circ}{T}\right)_{T=T} - \left(\frac{\Delta\mu_A^\circ}{T}\right)_{T=T_{m,A}} = \int_{T_{m,A}}^{T} \frac{\partial\Delta\mu_A^\circ}{\partial T}\,\partial T$$

Neglecting heat capacities and assuming the enthalpy of fusion of A, ΔH_A is approximately constant over this temperature range we get:

$$\left(\frac{\Delta\mu_A^\circ}{T}\right)_{T=T} - \left(\frac{\Delta\mu_A^\circ}{T}\right)_{T=T_{m,A}} = \Delta H_A\left[\frac{1}{T} - \frac{1}{T_{m,A}}\right]$$

or

$$R\ln(X_A) = \Delta H_A\left[\frac{1}{T_{m,A}} - \frac{1}{T}\right]$$

This is the usual depression of freezing point expression. The gradient of this line at $X_A \rightarrow 1$ is $RT_{m,A}^2/\Delta H$, that is, non-zero.

(B). Complex Formation. We can also consider the melting point behavior for the complexes A_mB_n. The result will depend upon the extent of complexation in the liquid state.

(B.1). Complex Formation: Complex Stable in Liquid and Solid. If the complex AB melts to form the liquid AB, then this essentially is behaving as if it were a pure compound. The melting point variation will therefore be the same as above for a pure

dx.doi.org/10.1021/la1048198 |Langmuir 2011, 27, 3626–3637

material; however, the mole fraction of the species A and AB will change reflecting this complexation. Essentially the phase diagram can be considered as two phase diagrams A and AB, and AB and B.

If we are on the $X_A < 0.5$ side of the phase diagram for an AB complex, the total number of species of A, N_{AT}, and B, N_{BT}, are given by

$$N_{AT} = N_{tot}X_A$$

$$N_{BT} = N_{tot}(1 - X_A)$$

If all the A is complexed to give AB, then the amount of AB, N_{AB}, will be

$$N_{AB} = N_{AT}$$

The amount of uncomplexed B remaining after some has been used to make the complex will therefore be

$$N_B = N_{BT} - N_{AT}$$

At this composition, only AB and uncomplexed B are present, and hence, the mole fraction of AB, X_{AB}, is therefore

$$\begin{aligned} X_{AB} &= N_{AB}/(N_{AB} + N_B) \\ &= N_{A,T}/(N_{A,T} + (N_{B,T} - N_{A,T})) = N_{A,T}/N_{B,T} \end{aligned}$$

The original mole fraction X_A is given by

$$X_A = N_{AT}/(N_{AT} + N_{AT})$$

So

$$X_{AB} = X_A/(1 - X_A)$$

On the A rich side of the phase diagram, this becomes

$$X_{AB} = (1 - X_A)/X_A$$

X'_A and X'_B are the new mole fractions of A and B when complex AB is included. If X_A is less than 0.5, then X'_A will be zero and X'_B will be given by

$$X'_B = (1 - 2X_A)/(1 - X_A)$$

If X_A is greater than 0.5, then X'_B will be zero and $X_A{}'$ will be given by

$$X'_B = (2X_A - 1)/X_A$$

(B.2). Complex Formation: Complex Stable in Solid but Dissociates in the Liquid. If the complex AB dissociates on melting, then we need to consider the equilibrium of the AB complex in the solid and A and B in the liquid.

$$AB(s) \leftrightarrow A(l) + B(l)$$

The condition for equilibrium is that

$$\sum v_i \mu_i = 0$$

where v is the stoichiometric coefficient of species m in equilibrium with products taken as positive and reactants as negative. μ_m is the chemical potential of species m.

For the equilibrium above, we have

$$\mu_A(l) + \mu_B(l) - \mu_{AB}(s) = 0$$

Here $\mu_{AB}(s)$ is per mole of AB. An alternative presentation considers $\mu_{AB}(s)$ as per mole of mixture (i.e., 1/2 mol of A and 1/2 mol of B in the liquid) and hence

$$\frac{1}{2}[\mu_A(l) + \mu_B(l)] = \mu_{AB}(s)$$

The final result below is independent of the approach taken and is reflected in the definition of the enthalpy of melting of the pure AB complex in the final expression, which will differ by a factor of 2.

Substituting for the chemical potentials of the liquid states as above.

$$\mu_A(l) = \mu_A^\circ(l) + RT\ln(X_A)$$

and

$$\mu_B(l) = \mu_B^\circ(l) + RT\ln(1 - X_A)$$

We obtain at general temperature T

$$\mu_A^\circ(l) + RT\ln(X_A) + \mu_B^\circ(l) + RT\ln(1 - X_A) = \mu_{AB}(s)$$

Taking

$$\Delta\mu_{AB}(T) = \mu_A^\circ(l) + \mu_B^\circ(l) - \mu_{AB}(s)$$

$$\frac{\Delta\mu_{AB}(T)}{T} = RT\ln(X_A) + R\ln(1 - X_A)$$

$$\frac{\Delta\mu_{AB}(T)}{T} = R\ln\big(X_A(1 - X_A)\big) \qquad (3)$$

at the melting point of the pure stoichiometic complex AB (for example), temperature $T_{m,AB}$, we have

$$\frac{\Delta\mu_{AB}(T_{m,AB})}{T_{m,AB}} = R\ln(1/4) \qquad (4)$$

Subtracting eq 4 from eq 3 as before

$$\frac{\Delta\mu_{AB}(T)}{T} - \frac{\Delta\mu_{AB}(T_{m,AB})}{T_{m,AB}} = R\ln(X_A(1 - X_A)) - R\ln(1/4)$$

$$\frac{\Delta\mu_{AB}(T)}{T} - \frac{\Delta\mu_{AB}(T_{m,AB})}{T_{m,AB}} = R\ln(4X_A(1 - X_A))$$

Using the Gibbs−Helmholtz equation and assuming the enthalpy of melting of the pure complex ΔH_{AB} is approximately constant with temperature as above, we obtain:

$$\Delta H_{AB}\left[\frac{1}{T} - \frac{1}{T_{m,AB}}\right] = R\ln\big(4X_A(1 - X_A)\big)$$

Or in terms of the temperature on the liquidus:

$$T = \frac{1}{\dfrac{1}{T_{m,AB}} - \dfrac{R}{\Delta H_{AB}}\ln\big(4X_A(1 - X_A)\big)}$$

We note that at the stoichiometric composition ($X_A = 1/2$) the gradient of this line is zero. This differs from the melting of the AB complex without dissociation where the gradient is nonzero and indicates that the phase diagram permits us to determine the extent of complexation in the liquid state.

(B.3). Complex Formation: General Stoichiometry A_mB_n. Similar considerations can be used to predict the melting behavior of A_2B and A_3B complexes assuming they remain associated in the liquid or dissociate to the A and B species. When they remain associated, we obtain a similar expression to

dx.doi.org/10.1021/la1048198 |Langmuir 2011, 27, 3626–3637

the normal pure material depression of freezing point. If the complexes dissociate, then we obtain a dependence of the form (see the Supporting Information):

$$T = \frac{1}{\frac{1}{T_m^{A_mB_n}} - \frac{R}{\Delta H_{A_mB_n}} \ln\left(\left(\frac{X_A(m+n)}{m}\right)^m \left(\frac{(1-X_A)(m+n)}{n}\right)^n\right)}$$

(C). Complex Formation: Complex of General Stoichiometry A_mB_n Stable in Solid but Dissociates in the Liquid. If the complex A_mB_n dissociates on melting, then we need to consider the equilibrium of the A_mB_n complex in the solid and A and B in the liquid.

$$A_mB_n(s) \leftrightarrow MA(l) + NB(l)$$

The condition for equilibrium is that

$$\Sigma v\mu_i = 0$$

where v is the stoichiometric coefficient of the species taken as positive for products and negative for reactants. μ_i is the chemical potential of species i.

For the equilibrium above we have,

$$M\mu_A(l) + N\mu_B(l) - \mu_{A_mB_n}(s) = 0$$

Substituting for the chemical potentials of the liquid states as above,

$$\mu_A(l) = \mu_A^\circ(l) + RT\ln(X_A) \quad \text{and} \quad \mu_B(l) = \mu_B^\circ(l) + RT\ln(1-X_A)$$

We obtain at general temperature T

$$M\mu_A^\circ(l) + MRT\ln(X_A) + N\mu_B^\circ(l) + NRT\ln(1-X_A) = \mu_{AB}(s)$$

Taking

$$\Delta\mu_{AB}(T) = \mu_A^\circ(l) + \mu_B^\circ(l) - \mu_{AB}(s)$$

we have

$$\frac{\Delta\mu_{AB}(T)}{T} = MR\ln(X_A) + NR\ln(1-X_A)$$

$$\frac{\Delta\mu_{AB}(T)}{T} = R\ln\left({X_A}^M(1-X_A)^N\right) \qquad (3)$$

At the melting point of the pure stoichiometic complex A_mB_n, temperature T_{m,A_mB_n}, we have $X_A = M/(M+N)$.

$$\frac{\Delta\mu_{AB}(T_{m,A_mB_n})}{T_{m,A_mB_n}} = R\ln\left(\left(\frac{M}{M+N}\right)^M\left(\frac{N}{M+N}\right)^N\right) \qquad (4)$$

Subtracting eqs 4 from 3 as before,

$$\frac{\Delta\mu_{AB}(T)}{T} - \frac{\Delta\mu_{AB}(T_{m,A_mB_n})}{T_{m,A_mB_n}} = R\ln({X_A}^M(1-X_A)^N) - R\ln\left(\left(\frac{M}{M+N}\right)^M\left(\frac{N}{M+N}\right)^N\right)\frac{\Delta\mu_{AB}(T)}{T}$$

$$-\frac{\Delta\mu_{AB}(T_{m,A_mB_n})}{T_{m,A_mB_n}} = R\ln\left(\left(\frac{(M+N)X_A}{M}\right)^M\left(\frac{(M+N)(1-X_A)}{N}\right)^N\right)$$

Using the Gibbs−Helmholtz equation and assuming the enthalpy of melting of the pure complex, $\Delta H_{A_mB_n}$ is approximately constant with temperature as above and we obtain:

$$\Delta H_{AB}\left[\frac{1}{T} - \frac{1}{T_{m,A_mB_n}}\right] = R\ln\left(\left(\frac{(M+N)X_A}{M}\right)^M\left(\frac{(M+N)(1-X_A)}{N}\right)^N\right)$$

Or in terms of the temperature of the liquidus:

$$T = \frac{1}{\frac{1}{T_{m,A_mB_n}} - \frac{R}{\Delta H_{A_mB_n}}\ln\left(\left(\frac{X_A(M+N)}{M}\right)^M\left(\frac{(1-X_A)(M+N)}{N}\right)^N\right)}$$

■ ASSOCIATED CONTENT

Supporting Information. Additional calorimetry data. This material is available free of charge via the Internet at http://pubs.acs.org.

■ AUTHOR INFORMATION

Corresponding Author

*E-mail: Stuart@bpi.cam.ac.uk. Telephone: 01223765706.

Present Addresses

‡Department of Chemistry, University of Liverpool, Crown Street, Liverpool L69 7ZD, United Kingdom.

■ ACKNOWLEDGMENT

We thank Felipe Garcia, Dominic Wright, and Ian Paterson for their loan of gloveboxes, Paul Wood for the use of the Stoe diffractometer, and Phillip Gallego for his patient glassblowing. Thanks to the PSI and DLS staff and scientists Antonio Cervellino, Fabia Gozzo, Chiu Tang, Stephen Thompson, Julia Parker, and Tom Arnold for beam time and technical support. This work is based on experiments performed at the Diamond Light Source, Abingdon, U.K. and the Swiss Light Source, Paul Scherrer Institute, Villigen, Switzerland. This work was carried out with the support of the Diamond Light Source. The research leading to these results has received funding from the European Community's Seventh Framework Programme (FP7/2007-2013) under Grant Agreement No. 226716.

■ REFERENCES

(1) Kohler, F.; Miksch, G.; Kainz, C.; Liebermann, E. *J. Phys. Chem.* **1972**, *76*, 2764.

(2) Kohler, F.; Gopal, R.; Gotze, G.; Atrops, H.; Demiriz, M. A.; Liebermann, E.; Wilhelm, E.; Ratkovics, F.; Palagy, B. *J. Phys. Chem.* **1981**, *85*, 2524–2529.

(3) Backlund, S.; Karlsson, S.; Sjoblom, J. *J. Dispersion Sci. Technol.* **1994**, *15*, 561.

(4) Backlund, S.; Friman, R.; Karlsson, S. *Colloids Surf., A* **1996**, *123*, 125.

(5) Karlsson, S.; Backlund, S.; Friman, R. *Colloid Polym. Sci.* **1999**, *278*, 8.

(6) Karlsson, S.; Friman, R.; Lindstrom, B.; Backlund, S. *J. Colloid Interface Sci.* **2001**, *243*, 241–247.

(7) Kohler, F.; Atrops, H.; Kalali, H.; Liebermann, E.; Wilhelm, E.; Ratkovics, F.; Salamon, T. *J. Phys. Chem.* **1981**, *85*, 2520–2524.
(8) Karlsson, S.; Backlund, S.; Friman, R. *Colloid Polym. Sci.* **2000**, *278*, 8–14.
(9) Kahn, A.; Margues, E. F. *Curr. Opin. Colloid Interface Sci.* **2000**, *4*, 402–410.
(10) Saeten, J. O.; Sjoblom, J.; Gestblom, B. *J. Phys. Chem.* **1991**, *95*, 1449–1453.
(11) Backlund, S.; Friman, R.; Karlsson, S. *Colloids Surf., A* **1997**, *123−124*, 125–133.
(12) Paivarinta, J.; Karlsson, S.; Hotokka, M.; Poso, A. *Chem. Phys. Lett.* **2000**, *327*, 420–424.
(13) Paivarinta, J.; Karlsson, S.; Poso, A.; Hotokka, M *Chem. Phys.* **2001**, *263*, 127–138.
(14) Epseau, P.; Reynolds, P. A.; Dowling, T.; Cookson, D.; White, J. *J. Chem. Soc., Faraday Trans.* **1997**, *93*, 3201–3208.
(15) Arnold, T.; Dong, C. C.; Thomas, R. K.; Castro, M. A.; Perdigon, A.; Clarke, S. M.; Inaba, A. *Phys. Chem. Chem. Phys.* **2002**, *4*, 3430–3435.
(16) Arnold, T.; Thomas, R. K.; Castro, M. A.; Clarke, S. M.; Messe, L.; Inaba, A. *Phys. Chem. Chem. Phys.* **2002**, *4*, 345–351.
(17) Groszek, A. J. *Proc. R. Soc. London* **1970**, *A314*, 473.
(18) Findenegg, G. H. *J. Chem. Soc., Faraday Trans. I* **1972**, *68*, 1799.
(19) Bien-Vogelsang, U.; Findenegg, G. H. *Colloids Surf.* **1986**, *21*, 469–481.
(20) Findenegg, G. H.; Koch, C.; Liphard, M. In *Adsorption of decanol from heptane at the solution graphite interface, Adsorption from Solution*, Conference in Honour of D. H. Everett, Bristol, Sept 8−10, 1982; Ottewill, R. H., Rochester, C. H., Smith, A. L., Eds.; Academic Press: Bristol, 1982.
(21) Messe, L.; Clarke, S. M.; Inaba, A.; Arnold, T.; Dong, C. C.; Thomas, R. K. *Langmuir* **2002**, *18*, 4010–4013.
(22) Messe, L.; Clarke, S. M.; Inaba, A.; Dong, C. C.; Thomas, R. K.; Castro, M. A.; Alba, M. *Langmuir* **2002**, *18*, 9429–9433.
(23) Messe, L.; Perdigon, A.; Clarke, S. M.; Inaba, A.; Castro, M. A. *J. Colloid Interface Sci.* **2002**, *266*, 19–27.
(24) Morishige, K.; Kato, T. *J. Chem. Phys.* **1999**, *111*, 7095–7102.
(25) Morishige, K.; Sakamoto, Y. *J. Chem. Phys.* **1995**, *103*, 2354.
(26) Findenegg, G. H. *J. Chem. Soc., Faraday Trans.* **1973**, *169*, 1069.
(27) Bickerstaffe, A. K.; Cheah, N. P.; Clarke, S. M.; Parker, J.; Perdigon, A.; Messe, L.; Inaba, A. *J. Phys. Chem. B* **2006**, *110*, 5570–5575.
(28) Bickerstaffe, A. K.; Messe, L.; Clarke, S. M.; Parker, J.; Perdigon, A.; Cheah, N. P.; Inaba, A. *Phys. Chem. Chem. Phys.* **2004**, *6*, 3545–3550.
(29) Cheah, N. P.; Messé, L.; Clarke, S. M. *J. Phys. Chem. B* **2004**, *108*, 4466–4469.
(30) Epseau, P.; White, J. *J. Chem. Soc., Faraday Trans.* **1997**, *93*, 3197–3200.
(31) Castro, M.; Clarke, S. M.; Inaba, A.; Arnold, T.; Thomas, R. K. *Phys. Chem. Chem. Phys.* **1999**, *1*, 5017–5023.
(32) Castro, M. A.; Clarke, S. M.; Inaba, A.; Arnold, T.; Thomas, R. K. *Phys. Chem. Chem. Phys.* **1999**, *1*, 5203–5207.
(33) Blauwhoff, P. M. M.; Versteeg, G. F.; Swaaij, W. P. M. v. *Chem. Eng. Sci.* **1984**, *39*, 207–225.
(34) Xu, S.; Wang, Y.; Frederick, D. O.; Mather, A. E. *Chem. Eng. Sci.* **1996**, *51*, 841–850.
(35) Von Sydow, E. *Acta Crystallogr.* **1955**, *8*, 810–813.
(36) Bond, A. D. *New J. Chem.* **2004**, *28*, 104–114.
(37) Lide, D. R. *CRC Handbook of Chemistry and Physics*, 81st ed.; CRC Press: New York, 2000.
(38) Domalski, E. S.; Hearing, E. D. *J. Phys. Chem. Ref. Data* **1996**, *25*, 1–525.
(39) Oonk, H. A. J. *Phase Theory: the Thermodynamics of Heterogeneous Equilibria*; Elsevier Scientific Publishing Company: Amsterdam, 1981; Vol. 3.
(40) Rabe, J. P. *Ultramicroscopy* **1992**, *42−44*, 41–54.
(41) Bickerstaffe, A. K.; Clarke, S. M. *Colloids Surf., A* **2007**, *298*, 80–82.
(42) Arnold, T.; Clarke, S. M. *Langmuir* **2008**, *24*, 3325.
(43) Alba, M. D.; Castro, M. A.; Clarke, S. M.; Medina, S.; Messe, L.; Millan, C.; Orta, M. M.; Perdigon-Aller, A. C. *J. Phys. Chem. C* **2009**, *113*, 3176–3180.
(44) Arnold, T. The adsorption of alkanes from their liquids and binary mixtures. Ph.D. Thesis, Oxford, Oxford, 2001.
(45) Messe, L.; Perdigon, A.; Clarke, S. M.; Inaba, A.; Arnold, T. *Langmuir* **2005**, *21*, 5085–5093.
(46) Parker, J. E.; Clarke, S. M. *Langmuir* **2008**, *24*, 4833–4844.
(47) Parker, J. E.; Clarke, S. M.; Perdigon, A. C. *Surf. Sci.* **2007**, *601*, 4149–4153.
(48) Bhinde, T.; Clarke, S. M.; Phillips, T. K.; Arnold, T.; Parker, J. E. *Langmuir* **2010**, *26*, 8201–8206.
(49) Clarke, S. M.; Messe, L.; Adams, J.; Inaba, A.; Arnold, T.; Thomas, R. K. *Chem. Phys. Lett.* **2003**, *373*, 480–485.